International Journal of Engineering and Emerging Scientific Discovery
ISSN: 2536-7250 (Print): 2536-7269 (Online)
Volume 5, Number 1, March 2020
http://www.casirmediapublishing.com

THEORETICAL INVESTIGATION OF AN IMPACT OF LEFT-HANDED MATERIALS IN SURFACE PLASMON AND PROPAGATION LENGTH

[1]E. W. Likta, [2]O. W. Olosaji & [2]A. M. Tijjani
[1]Department of Physics, University of Maiduguri, Maiduguri, Borno State
[2]Department of Physics, Abubakar Tafawa Balewa University, Bauchi
E-Mail: emmalikta2014@gmail.com
Correspondence: [1]E. W. Likta

ABSTRACT
The goal of this paper is to obtain a theoretical investigation of surface plasmons of geometry. The studied shows the effect of LHM on the surface Plasmon propagation length. A Left-Handed Material layer excite surface plasma with lower energy dissipation rate allow longer propagation distance has been achieved.
Keywords: Surface plasma, LHM layer, Maxwell's equations, propagation and electric field

INTRODUCTION
The charge density oscillations and associated electromagnetic fields are called surface plasmon-polariton waves. The exponential dependence of the electromagnetic field intensity on the distance away from the interface is shown on the right. These waves can be excited very efficiently with light in the visible range of the electromagnetic spectrum. Surface plasmons (SPs) are coherent delocalized electron oscillations that exist at the interface between any two materials where the real part of the dielectric function changes signs across the interface (e.g. a metal-dielectric interface, such as a metal sheet in air). SPs have lower energy than bulk (or volume) plasmons which quantise the longitudinal electron oscillations about positive ion cores within the bulk of an electron gas (or plasma). The charge motion in a surface plasmon always creates electromagnetic fields outside (as well as inside) the metal. The total excitation, including both the charge motion and associated electromagnetic field, is called either a surface Plasmon polariton at a planar interface, or a localized surface plasmon for the closed surface of a small particle (Ritchie, 1957). In the following two decades, surface plasmons were extensively studied by many scientists. Information transfer in nanoscale structures, similar to photonics, by means of surface plasmons, is referred to as plasmonics (Polman et al., 2005). Surface plasmon polaritons can be excited by electrons or photons. In the case of photons, it cannot be done

directly, but requires a prism, or a grating, or a defect on the metal surface. At low frequency, an SPP approaches a Sommerfeld-Zenneck wave, where the dispersion relation (relation between frequency and wavevector) is the same as in free space. At a higher frequency, the dispersion relation bends over and reaches an asymptotic limit called the "surface plasma frequency". As an SPP propagates along the surface, it loses energy to the metal due to absorption. It can also lose energy due to scattering into free-space or into other directions. The electric field falls off evanescently perpendicular to the metal surface. At low frequencies, the SPP penetration depth into the metal is commonly approximated using the skin depth formula. In the dielectric, the field will fall off far more slowly. SPPs are very sensitive to slight perturbations within the skin depth and because of this, SPPs are often used to probe in homogeneities of a surface. For more details see surface Plasmon polariton.

The excitation of surface plasmons is frequently used in an experimental technique known as surface plasmon resonance (SPR). In SPR, the maximum excitation of surface plasmons are detected by monitoring the reflected power from a prism coupler as a function of incident angle or wavelength. This technique can be used to observe nanometer changes in thickness, density fluctuations, or molecular absorption. Surface plasmon-based circuits have been proposed as a means of overcoming the size limitations of photonic circuits for use in high performance data processing nano devices (Ozbay et al., 2006). The ability to dynamically control the plasmonic properties of materials in these nano-devices is key to their development. A new approach that uses plasmon-plasmon interactions has been demonstrated recently. Here the bulk plasmon resonance is induced or suppressed to manipulate the propagation of light (Akimov et al., 2012). This approach has been shown to have a high potential for nanoscale light manipulation and the development of a fully CMOS- compatible electro-optical plasmonic modulator, said to be a future key component in chip-scale photonic circuits (Wenshan et al., 2009). Some other surface effects such as surface- enhanced Raman scattering and surface- enhanced fluorescence are induced by surface plasmon of noble metals therefore sensors based on surface plasmon were developed (Xu et al., 2019).

In surface second harmonic generation, the second harmonic signal is proportional to the square of the electric field. The electric field is stronger at

International Journal of Engineering and Emerging Scientific Discovery
ISSN: 2536-7250 (Print): 2536-7269 (Online)
Volume 5, Number 1, March 2020
http://www.casirmediapublishing.com

the interface because of the surface plasmon resulting in a non-linear optical effect. This larger signal is often exploited to produce a stronger second harmonic signal (Valev, 2012). The wavelength and intensity of the plasmon-related absorption and emission peaks are affected by molecular adsorption that can be used in molecular sensors. For example, a fully operational prototype device detecting casein in milk has been fabricated. The device is based on monitoring changes in plasmon- related absorption of light by a gold layer (Minh et al., 2007).

MATERIALS AND METHODS

The propagating along x-direction and decaying along z direction as schematically as shown in figure below. In layer 2 $(z > 0)$, electric and magnetic fields are

$$H_{(2)} = \hat{y}Ae^{-jk_x^{(2)}x - k_z^{(2)}z + j\omega t} \quad 1$$

$$E_{(2)} = \left(\frac{A}{j\omega\varepsilon_0\varepsilon_{(2)}}\right)\left(\hat{x}k_z^{(2)} - \hat{z}k_z^{(2)}\right)e^{-jk_x^{(2)}x - k_z^{(2)}z + j\omega t} \quad 2$$

In layer 1 $(z < 0)$

$$H_{(1)} = \hat{y}Be^{-jk_x^{(1)}x + k_z^{(1)}z + j\omega t} \quad 3$$

$$E_{(1)} = \left(-\frac{B}{j\omega\varepsilon_0\varepsilon_{(1)}}\right)\left(\hat{x}k_z^{(1)} + \hat{z}k_z^{(1)}\right)e^{-jk_x^{(1)}x - k_z^{(1)}z + j\omega t} \quad 4$$

Where $k_z^{(1,2)}$ determines the decay in electromagnetic fields in Layer 1 and 2 which could be determined from the Maxwell's equation

$$\nabla^2 H - \frac{\mu_r\varepsilon_r}{c^2}\frac{\partial^2 H}{\partial t^2} = 0 \quad 5$$

Inserting $H_{(1)}$ *and* $H_{(2)}$ we have two conditions

$$-\left(k_x^{(2)}\right)^2 + \left(k_z^{(2)}\right)^2 + \left(\frac{\omega}{c}\right)^2\mu_{(2)}\varepsilon_{(2)} = 0 \quad 6$$

$$-\left(k_x^{(1)}\right)^2 + \left(k_z^{(1)}\right)^2 + \left(\frac{\omega}{c}\right)^2\mu_{(1)}\varepsilon_{(1)} = 0 \quad 7$$

Assuming there is no charge and current source in the system, boundary conditions, implying the fact that the tangential components of electric and magnetic fields at the interface should be continuous, yields:

$$A = B \quad A\frac{k_z^{(2)}}{\varepsilon_{(2)}} = -B\frac{k_z^{(1)}}{\varepsilon_{(1)}} \rightarrow \frac{k_z^{(1)}}{k_z^{(2)}} = -\frac{\varepsilon_{(1)}}{\varepsilon_{(2)}} \quad 8$$

SP dispersion $k_{sp} = k_z^{(1,2)}$ for the polarized incident wave is found as

$$k_{sp} = \frac{\omega}{c}\sqrt{\frac{\varepsilon_{(2)}\varepsilon_{(2)}\left(\varepsilon_{(1)}\mu_{(2)} - \varepsilon_{(2)}\mu_{(1)}\right)}{\left(\varepsilon_{(1)}^2 - \varepsilon_{(2)}^2\right)}} \quad 9$$

For a polarized light source, in Layer 2 ($z > 0$) electric and magnetic fields are

$$E_{(2)} = \hat{y}Ae^{-jk_x^{(2)}x - k_z^{(2)}z + j\omega t} \quad (10)$$

$$H_{(2)} = \left(\frac{A}{j\omega\varepsilon_0\varepsilon_{(2)}}\right)\left(\hat{x}k_z^{(2)} - \hat{z}k_z^{(2)}\right)e^{-jk_x^{(2)}x - k_z^{(2)}z + j\omega t} \quad (11)$$

In Layer 1 ($z < 0$)

$$E_{(1)} = \hat{y}Be^{-jk_x^{(1)}x + k_z^{(1)}z + j\omega t} \quad (12)$$

$$H_{(1)} = \left(-\frac{B}{j\omega\varepsilon_0\varepsilon_{(1)}}\right)\left(\hat{x}k_z^{(1)} + \hat{z}k_z^{(1)}\right)e^{-jk_x^{(1)}x - k_z^{(1)}z + j\omega t} \quad (13)$$

From the Maxwell's equations

$$\nabla^2 E - \frac{\mu_r\varepsilon_r}{c^2}\frac{\partial^2 E}{\partial t^2} = 0 \quad (14)$$

Inserting $H_{(1)}$ *and* $H_{(2)}$ we have two conditions

$$-\left(k_x^{(2)}\right)^2 + \left(k_z^{(2)}\right)^2 + \left(\frac{\omega}{c}\right)^2\mu_{(2)}\varepsilon_{(2)} = 0 \quad (15)$$

$$-\left(k_x^{(1)}\right)^2 + \left(k_z^{(1)}\right)^2 + \left(\frac{\omega}{c}\right)^2\mu_{(1)}\varepsilon_{(1)} = 0 \quad (16)$$

Assuming again there is no charge and current source in the system, applying the same boundary the conditions yields

$$A = B \quad A\frac{k_z^{(2)}}{\mu_{(2)}} = B\frac{k_z^{(1)}}{\mu_{(1)}} \rightarrow \frac{k_z^{(1)}}{k_z^{(2)}} = -\frac{\mu_{(1)}}{\mu_{(2)}} \quad (17)$$

SP dispersion $k_{sp} = k_z^{(1,2)}$ for the polarized incident wave is found as

$$k_{sp} = \frac{\omega}{c}\sqrt{\frac{\mu_{(2)}\mu_{(2)}\left(\varepsilon_{(2)}\mu_{(1)} - \varepsilon_{(1)}\mu_{(2)}\right)}{\left(\mu_{(1)}^2 - \mu_{(2)}^2\right)}} \quad (18)$$

The electric field in Layer 2 can be written as

$$E_{(2)} = \hat{y}e^{jk_x^{(2)}x}\left(A_{(2)}e^{jk_z^{(2)}z} + B_{(2)}e^{-jk_z^{(2)}z}\right) \quad (19)$$

where $B_{(2)}$ is the amplitude of the wave (Dural, 1995). The electric field in Layer 2 can be written as

$$E_{(1)} = \hat{y}A_{(2)}e^{jk_x^{(2)}x}\left(e^{jk_z^{(2)}z} + \tilde{R}_{2,1}e^{-jk_z^{(2)}z}\right) \quad (20)$$

The electric field in the layer is written as

$$E_{(1)} = \hat{y}A_{(1)}e^{jk_x^{(2)}x}\left(e^{jk_z^{(2)}z} + R_{1,0}e^{-jk_z^{(2)}(z+2d)}\right) \quad (21)$$

The amplitude transfer Layer 2 and 1 for the down-going waves can be written as

$$A_{(1)} = A_{(2)}T_{2,1} + A_{(1)}R_{1,0}e^{-jk_z^{(2)}2d}R_{1,2} \quad (22)$$

Rearranging the terms, amplitude $A_{(1)}$ can be written in terms of $A_{(2)}$ as

International Journal of Engineering and Emerging Scientific Discovery
ISSN: 2536-7250 (Print): 2536-7269 (Online)
Volume 5, Number 1, March 2020
http://www.casirmediapublishing.com

$$A_{(1)} = A_{(2)} \frac{T_{2,1}}{1-R_{1,0}R_{1,2}\, e^{-jk_z^{(1)}2d}} \quad 23$$

The amplitude transfer between Layer 2 and 1 for the up-going waves can be written as

$$A_{(1)}\tilde{R}_{2,1} = A_{(2)}R_{2,1} + A_{(1)}R_{1,0}e^{-jk_z^{(1)}2d}T_{1,2} \quad 24$$

Results and Discussion

Generalizing the reflection coefficient $\tilde{R}_{2,1}$ between Layer 1 and 2 is found as

$$\tilde{R}_{2,1} = R_{2,1} + \frac{T_{1,2}T_{2,1}R_{1,0}e^{-jk_z^{(1)}2d}}{1-R_{1,0}R_{1,2}\, e^{-jk_z^{(1)}2d}} \quad 25$$

Where reflection $(R_{i+1,i})$ and transmission $(T_{i+1,i})$ coefficients are

$$R_{i+1,i} = \frac{\sqrt{\varepsilon_{i+1}}\cos\theta_i - \sqrt{\varepsilon_i}\sqrt{1-\frac{\varepsilon_i}{\varepsilon_{i+1}}\sin^2\theta_i}}{\sqrt{\varepsilon_{i+1}}\cos\theta_i + \sqrt{\varepsilon_i}\sqrt{1-\frac{\varepsilon_i}{\varepsilon_{i+1}}\sin^2\theta_i}} \qquad T_{i+1,i} = 1 + R_{i+1,i} \quad 26$$

For the incidence angle greater than θ_c, $\sin\theta_c = \sqrt{\frac{\mu_1\varepsilon_1}{\mu_2\varepsilon_2}}$ supporting information text for the derivation of the critical angle

$$R_{i+1,i} = \frac{\cos\theta_i - j\sqrt{\sin^2\theta_i - \frac{\varepsilon_i}{\varepsilon_{i+1}}}}{\cos\theta_i + j\sqrt{\sin^2\theta_i - \frac{\varepsilon_i}{\varepsilon_{i+1}}}} \quad 27$$

Taking the imaginary part of SP wave vector the part corresponds to the energy dissipation

$$L_{sp} = \frac{1}{2k''_{sp}} \quad 28$$

Using permittivity and permeability functions can written

$$\varepsilon_{(2)} = 1 - \frac{\omega_{pL}^2}{\omega - j\gamma} \quad 29$$

$$\mu_{(2)} = 1 - \frac{F\omega_0^2}{\omega^2 - \omega_0^2 - j\Gamma_L\omega} \quad 30$$

where ω_{pL} is the plasma frequency, γ is the damping parameter, F is a parameter between 0 and 1, Γ_L is the scattering rate and ω_0 is the frequency at which effective permeability. The frequency dependent permittivity of the metal is determined by Drude model

$$\varepsilon_{(2)} = 1 - \frac{\omega_p^2}{\omega^2 - j\Gamma\omega} \quad 31$$

where ω_p is the plasma frequency of the metal and Γ is the scattering rate.

Table 1: Electric field distribution and a distance of propagation

S/N	$\|E\|$	$\mu(m)$
1	1.0	0.00
2	0.9	0.05
3	1.0	0.10
4	0.9	0.15
5	1.0	0.20
6	0.9	0.25
7	1.0	0.30
8	0.9	0.35
9	1.0	0.40
10	0.9	0.45
11	1.0	0.50
12	0.9	0.55
13	1.0	0.60
14	0.9	0.65
15	1.0	0.70
16	0.9	0.75
17	1.0	0.80
18	0.9	0.85
19	1.0	0.90
20	0.9	0.95
21	1.0	1.00
22	0.9	1.05
23	1.0	1.10
24	0.9	1.15
25	1.0	1.20
26	0.9	1.25
27	1.0	1.30
28	0.9	1.35
29	1.0	1.40
30	0.9	1.45
31	1.0	1.50
32	2.9	1.80
33	0.0	1.95

International Journal of Engineering and Emerging Scientific Discovery
ISSN: 2536-7250 (Print): 2536-7269 (Online)
Volume 5, Number 1, March 2020
http://www.casirmediapublishing.com

Table 2: Reflection and angle of incidence of a dielectric

S/N	Reflection	Angle of incidence (°)
1	0.70	0.00
2	0.65	2.00
3	0.80	10.00
4	0.85	15.00
5	0.90	16.00
6	0.85	17.00
7	0.00	18.00
8	0.85	19.00
9	1.00	20.00
10	1.00	40.00
11	1.00	60.00
12	1.00	80.00

Table 3: Surface Plasmon propagation length with respect to the change in the permittivity and permeability of the wavelength

S/N	$L_{SP}(nm)$	Wavelength (nm)	ϵ_{metal}	Wavelength (nm)	μ_{LHM}	Wavelength (nm)	ϵ_{LHM}	Wavelength (nm)
1	10.0	0.00	-11.0	0.00	-0.05	0.00	-7.5	0.00
2	10.0	1050	-10.5	1050	-0.05	1050	-7.0	1050
3	10.0	1100	-10.0	1100	-0.05	1100	-7.0	1100
4	10.0	1150	-9.5	1150	-0.10	1150	-6.5	1150
5	10.0	1200	-9.5	1200	-19.00	1200	-6.0	1200
6	55.0	1250	-9.0	1250	-0.10	1250	-5.5	1250
7	101	1300	-8.5	1300	-0.05	1300	-5.0	1300
8	100	1325	-8.0	1325	-0.05	1325	-4.5	1325

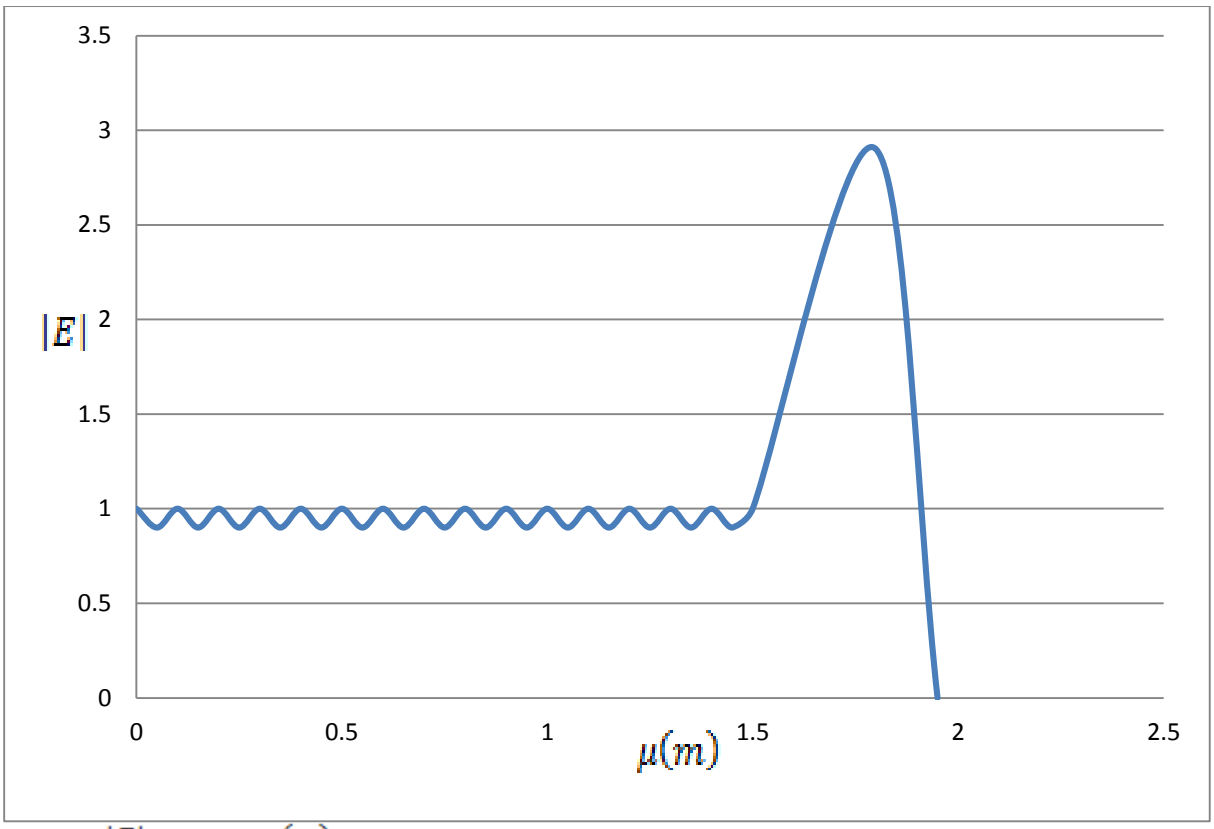

Fig. 1: $|E|$ versus $\mu(m)$

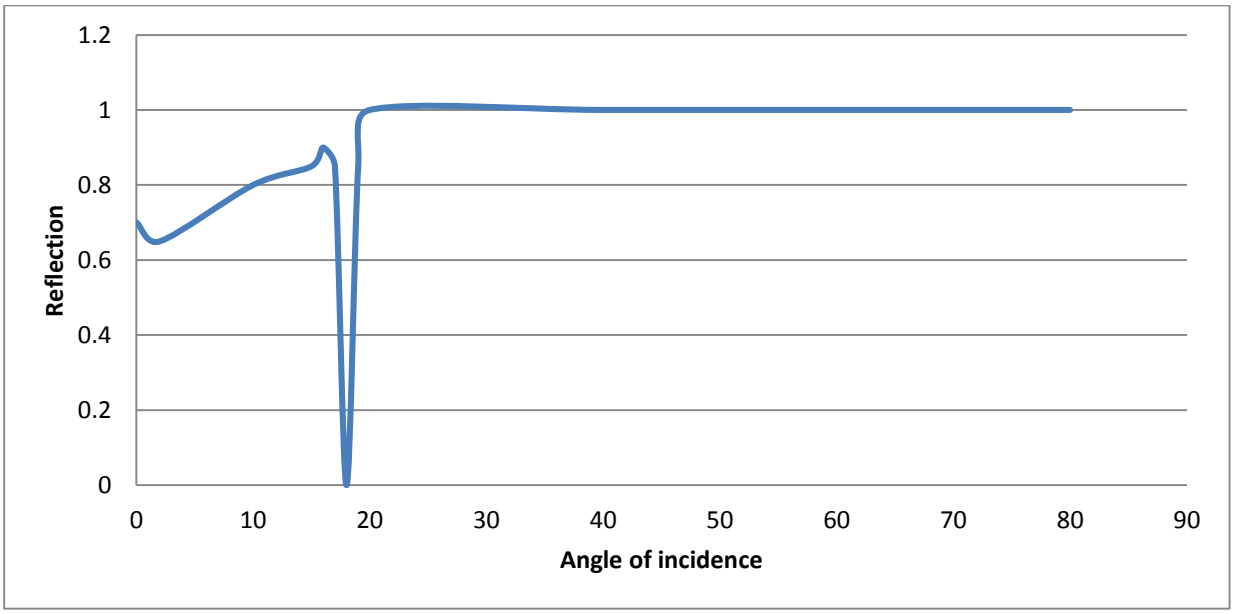

Fig2: Reflection versus Angle of incidence

International Journal of Engineering and Emerging Scientific Discovery
ISSN: 2536-7250 (Print): 2536-7269 (Online)
Volume 5, Number 1, March 2020
http://www.casirmediapublishing.com

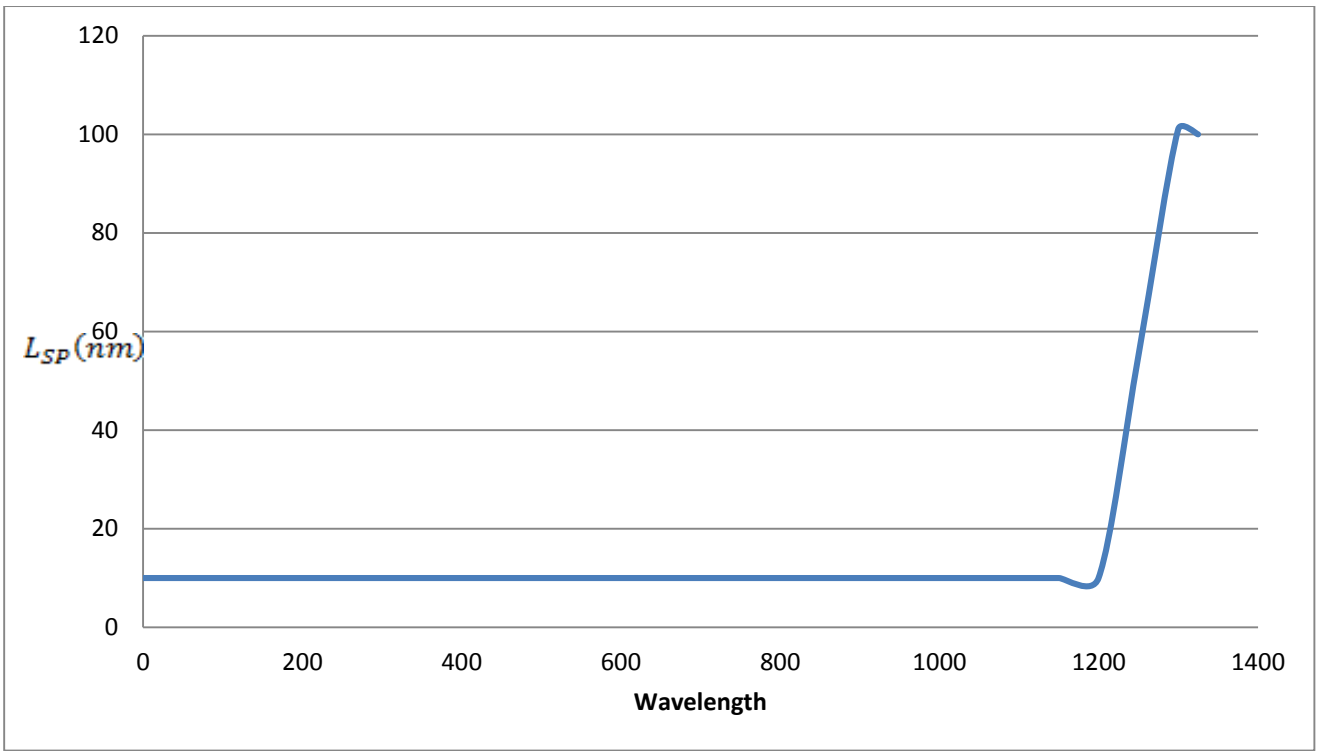

Fig 3a: $L_{SP}(nm)$ versus Wavelength

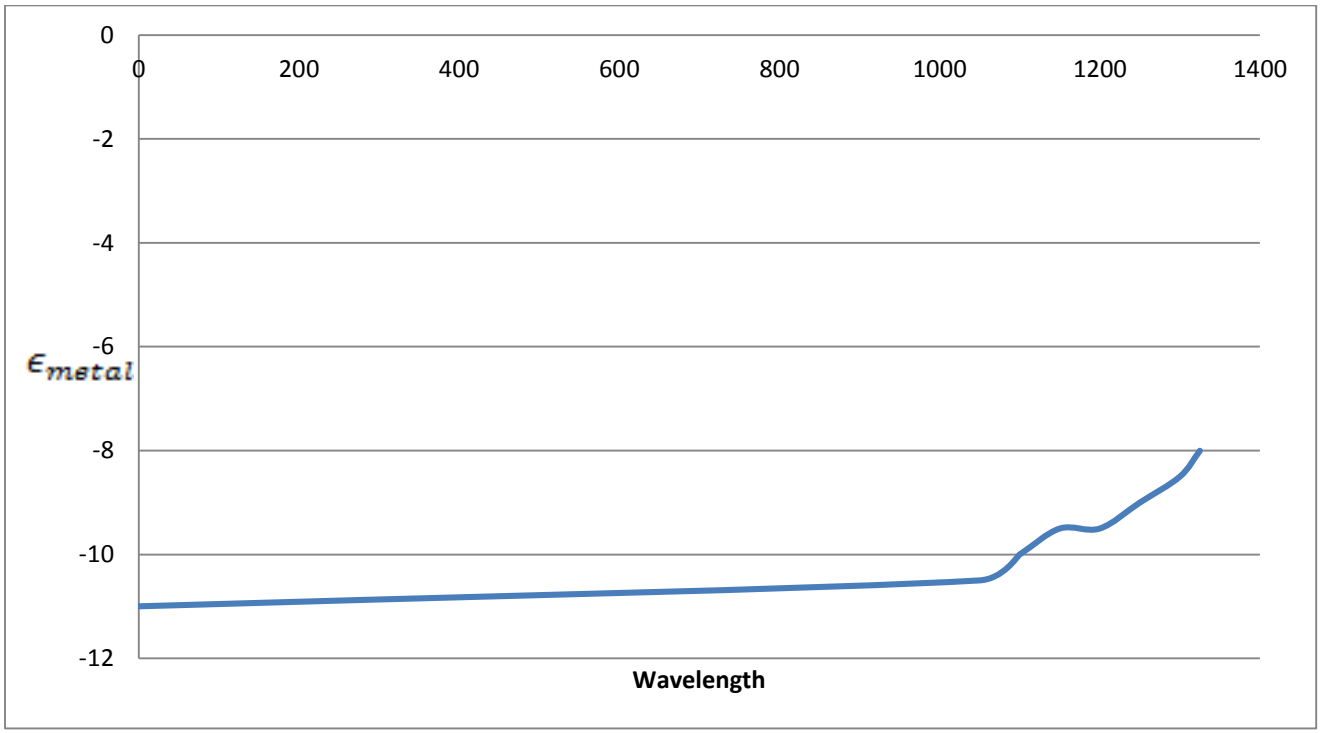

Fig3: ϵ_{metal} versus Wavelength

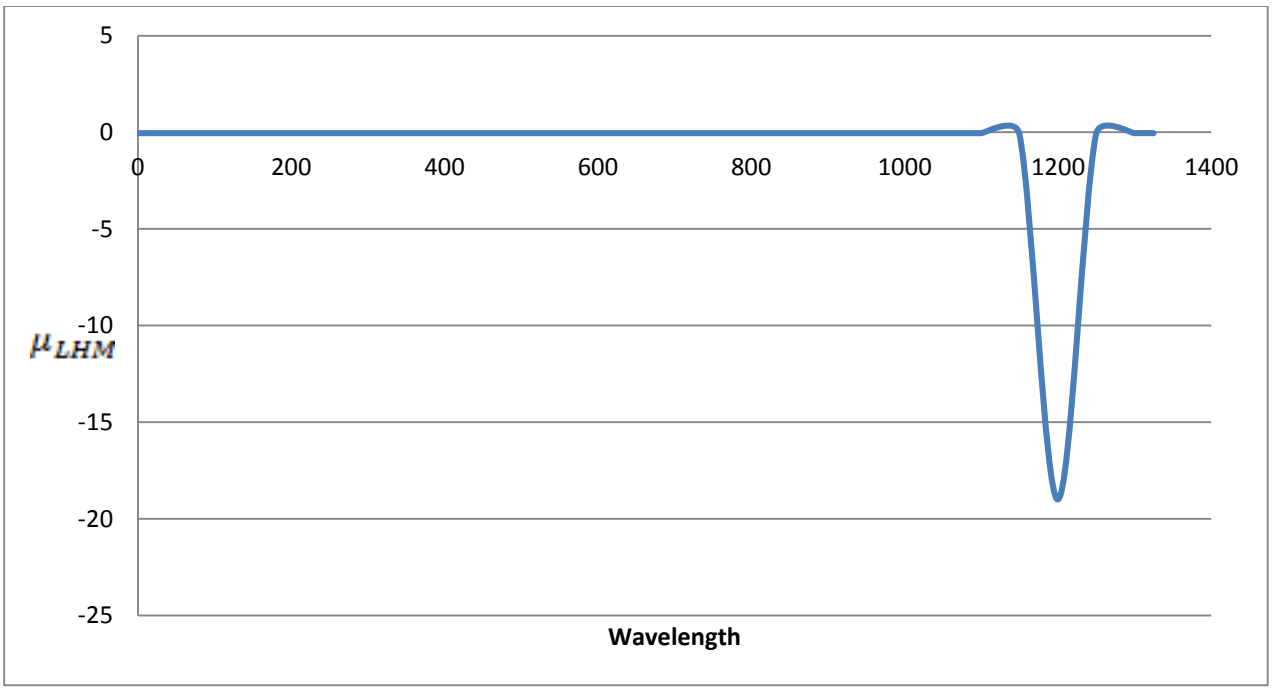

Fig. 3c: μ_{LHM} versus Wavelength

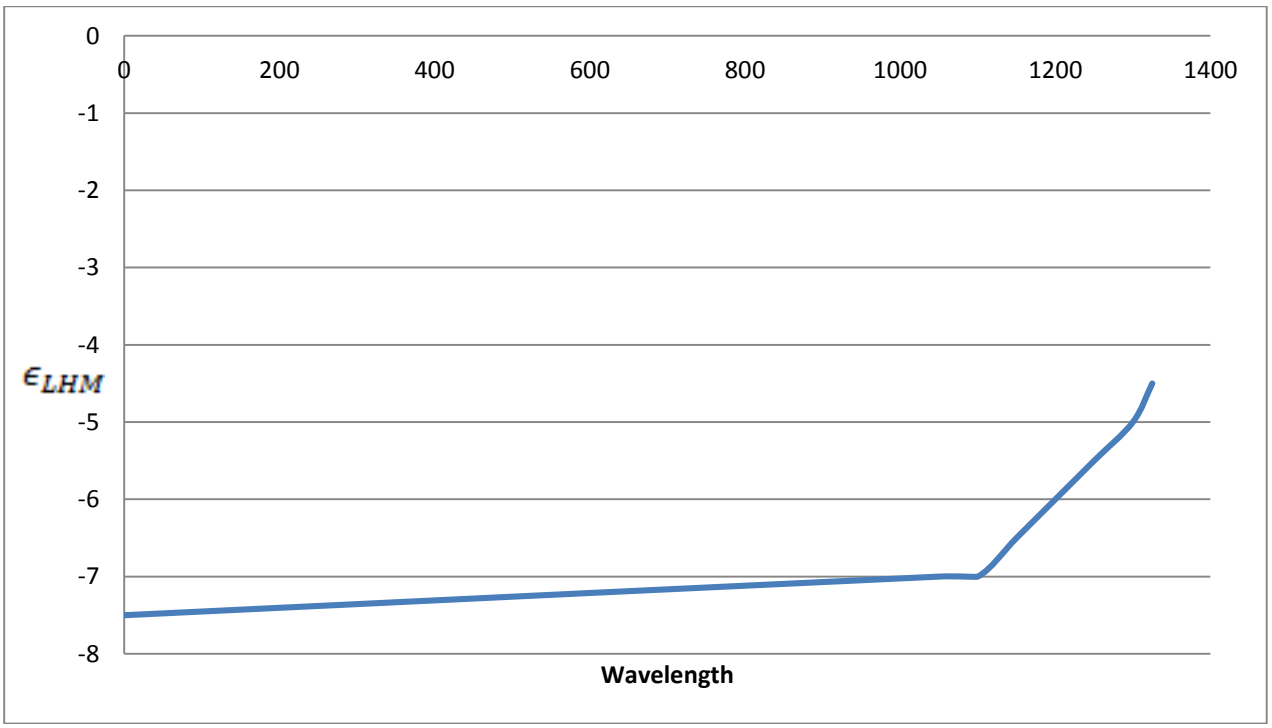

Fig. 3d: ϵ_{LHM} versus Wavelength

Fig.1 shows that surface waves propagate on surface and they vanish along the directions normal to it, the wave along the interface between LHM and

International Journal of Engineering and Emerging Scientific Discovery
ISSN: 2536-7250 (Print): 2536-7269 (Online)
Volume 5, Number 1, March 2020
http://www.casirmediapublishing.com

metal layer decay and the distribution of electric field as a function of distance along the propagation direction.

Fig.2 shows that the calculated generalized reflection coefficient and the reflection amplitude was determined from FEM simulation. Which the reflection is calculated by fitting a sum of experimental in the GPOF method, the calculated results and the simulation results shows good agreement to each other.

Fig. 3 a, b, c and d shows the permittivity and permeability of the LHM and metal layer. These demonstrate that the LHM layer has negative permittivity and permeability while the surface plasma propagation length increases. An improvement in the excitation of the vanish field along the medium above the metal layer which create stronger surface waves that can propagate longer distance before their energy.

CONCLUSION

The dispersion relation of surface plasma creates along a LHM metal interface has been studied. Light polarizations enabling surface plasma excitation through LHM platforms and proved that the unlike classical scheme with LHM, surface plasma is excited through a polarized incident light source which has been investigated. The negative permittivity and permeability of LHM layer can excite surface plasma. Surface plasma in periodic metallic system could propagate longer wavelength while experimental realization covers plasmonic surface. The theoretical and experimental result shows good agreement to each other.

REFERENCE

Akimov, Y. A and Chu, H S (2012): Plasmon–plasmon interaction: Controlling light at nanoscale. Nanotechnology. 23 (44): 44-49.

Dural Z (1995): Waves and fields in Inhomogeneous Media New York, USA, Springer-Velag, Vol. 302, pp 131-137.

Minh H. H., Endo T. and Kerman K. (2007): A localized surface plasmon resonance based immunosensor for the detection of casein in milk. Science and Technology of Advanced Materials. 8 (4): 331.

Ozbay, E. (2006): Plasmonics, Merging Photonics and Electronics at Nanoscale Dimensions. Science. 311 (5758): 189–93.

Polman, A and Harry A. A (2005): Plasmonics: optics at the nanoscale. Materials Today. 8: 56.

Ritchie, R. H. (1957): Plasma Losses by Fast Electrons in Thin Films. Physical Review. 106 (5): 874–881.

Valev V. K. (2012): Characterization of Nanostructured Plasmonic Surfaces with Second Harmonic Generation. Langmuir. 28 (44): 15454–15471.

Wenshan C., Justin S. W. and Mark L. Brongersma (2009): Compact, High-Speed and Power-Efficient Electrooptic Plasmonic Modulators. Nano Letters. 9 (12): 4403– 11.

Xu Z., Chen, Y., Gartia M., Jiang J. and Liu L. (2019):Surface Plasmon enhanced broadband spectrophotometry on black silver substrates". Applied Physics Letters. 98 (24): 24-40.